Video Article

# Non-invasive Parenchymal, Vascular and Metabolic High-frequency Ultrasound and Photoacoustic Rat Deep Brain Imaging

Pierangela Giustetto[1,2], Miriam Filippi[2], Mauro Castano[3], Enzo Terreno[1,2]

[1]Center for Preclinical Imaging, Department of Molecular Biotechnology and Health Sciences, University of Turin

[2]Molecular Imaging Center, Department of Molecular Biotechnology and Health Sciences, University of Turin

[3]Bracco Research Center, Bracco Imaging SpA

Correspondence to: Pierangela Giustetto at pierangela.giustetto@unito.it

URL: http://www.jove.com/video/52162
DOI: doi:10.3791/52162

Keywords: Neuroscience, Issue 97, Photoacoustics, High-frequency ultrasounds, Brain imaging, Cerebral hemodynamics, Non-invasive imaging, Small animal, Neuroimaging

Date Published: 3/2/2015

Citation: Giustetto, P., Filippi, M., Castano, M., Terreno, E. Non-invasive Parenchymal, Vascular and Metabolic High-frequency Ultrasound and Photoacoustic Rat Deep Brain Imaging. *J. Vis. Exp.* (97), e52162, doi:10.3791/52162 (2015).

## Abstract

Photoacoustics and high frequency ultrasound stands out as powerful tools for neurobiological applications enabling high-resolution imaging on the central nervous system of small animals. However, transdermal and transcranial neuroimaging is frequently affected by low sensitivity, image aberrations and loss of space resolution, requiring scalp or even skull removal before imaging. To overcome this challenge, a new protocol is presented to gain significant insights in brain hemodynamics by photoacoustic and high-frequency ultrasounds imaging with the animal skin and skull intact. The procedure relies on the passage of ultrasound (US) waves and laser directly through the fissures that are naturally present on the animal cranium. By juxtaposing the imaging transducer device exactly in correspondence to these selected areas where the skull has a reduced thickness or is totally absent, one can acquire high quality deep images and explore internal brain regions that are usually difficult to anatomically or functionally describe without an invasive approach. By applying this experimental procedure, significant data can be collected in both sonic and optoacoustic modalities, enabling to image the parenchymal and the vascular anatomy far below the head surface. Deep brain features such as parenchymal convolutions and fissures separating the lobes were clearly visible. Moreover, the configuration of large and small blood vessels was imaged at several millimeters of depth, and precise information were collected about blood fluxes, vascular stream velocities and the hemoglobin chemical state. This repertoire of data could be crucial in several research contests, ranging from brain vascular disease studies to experimental techniques involving the systemic administration of exogenous chemicals or other objects endowed with imaging contrast enhancement properties. In conclusion, thanks to the presented protocol, the US and PA techniques become an attractive noninvasive performance-competitive means for cortical and internal brain imaging, retaining a significant potential in many neurologic fields.

## Video Link

The video component of this article can be found at http://www.jove.com/video/52162/

## Introduction

Strategies to minutely describe features of brain hemodynamics in the central nervous system of small animals are needed to advance the field of neuroscience[1-3]. The presented technique demonstrates how to perform noninvasive acoustic and photoacoustic imaging on small animal brain in order to examine vascular biology, arrangement and function.

Optical imaging techniques allow localization of events related to neural activity[2,4-5] and simultaneously acquire signals generated by hemoglobin both in oxygenated and non-oxygenated states[6]. However, due to photonic absorption and scattering, pure optical imaging suffers from poor spatial resolution and limited tissue penetration depth[7-8]. Conversely, acoustics offer the opportunity to perform deeper imaging with higher space spatial resolution, but it is hindered by speckle and limited contrast[9-11]. By combining features of photonics with ultrasound, photoacoustic technique improves both imaging and diagnostic potentialities of single methods[12-16].

Photoacoustic imaging of the brain has the potential to elucidate multiple questions in neurobiology, however, the skullcap that naturally protects the encephalon, dramatically limits both the photonic and ultrasonic tissue penetration[17-19]. Moreover, bones promote scattering of both light and sound resulting in loss of sensitivity and image aberrations[17-18]. As a consequence, brain ultrasonic and photoacoustic imaging can be easily performed on neonate animals prior to ossification[20], but the deep anatomy and physiology of the adult brain are clearly accessible only after craniotomy[21,22]. Regrettably, the surgery needed for skull removal is technically hard and its effects can be detrimental for some experimental purposes thus making it difficult to monitor neural disease progression in the same animal over time. Therefore, a non-invasive method to image deep cerebral biology in small animal models is highly desirable. In the literature the method of photon recycler[17] is reported as a way to reduce the phone loss and increase the transmittance through the intact skull, improving the photoacoustic signal to noise ratio (SNR) and the contrast of the target.

The presented protocol aims to provide a reliable method for subcortical brain acoustic and photoacoustic imaging on research-use rodents (specifically on rats) without any invasive surgery. The procedure is based on the use of portable transducing devices for high-frequency ultrasound and photoacoustic imaging. In contrast to tomographic imaging technology[23], portable and directional transducers[24] enable selection of specific cranium regions with naturally reduced thickness, termed fissures or scissures. The major clefts (foramina) present on the vertebrate animal skull are necessary to locate the nerve bundles, vessels or other structures connecting internal encephalon circuits to other parts of the body. The major clefts are found in differently sized bone openings that can be exploited as specific passages for ultrasound waves and laser. Such targeted imaging reduces wave reflection effects caused by bone interfaces and increases sensitivity by enhancing the imaging penetration depth. In this perspective, the imaging transducer can be arranged to be perpendicular to the clefts located on the temporal and on the occipital side of the skull (**Figure 1**), in order to maximally converge the ultrasound and photonic beams on these areas. This orientation both enhances signal quality and forces the signal to proceed through a thinner bone layer with respect to other cranial orientations. Thus, the transmitted and reflected waves undergo a lower degree of scattering, enabling collection of intense signals originating from deeper tissue layers. In contrast to earlier procedures, this experimental setting requires just animal head shaving, while no other surgery is necessary.

With the proposed protocol, imaging is performed at relatively high spatial resolution, revealing both, specific reference anatomic structures and blood vessels deeper than current state of art methods, all while the animal skin and skull remain intact. Unique coronal and axial images can be acquired by exploiting various ultrasonic imaging acquisition modalities (B, Power Doppler, Color Doppler, Pulsed Wave Mode) in parallel to photoacoustic imaging. An extended repertoire of parameters can be extracted from these images, enabling depiction of parenchymal and vascular anatomy alongside an entire collection of features affecting blood circulation dynamics. This protocol can be used to image basic cortical parenchyma features in High Frequency Ultrasonic B Mode modality, the basilar and internal carotid arteries (BA and ICA respectively) composing the Circle of Willis, the Middle Cerebral Artery (MCA) and other details of the circulatory apparatus. Further, blood flow quantification, mean stream velocities, directional motion description and oxygen saturation data can be collected from cortical to deep brain regions.

This new strategy holds great potential for a variety of applications and satisfies the urgent need for reliable procedures to depict deep brain features that are crucial in various pathologies. Furthermore, because of its minimal invasiveness, the presented protocol can enable myriad possible imaging studies on the central nervous system, particularly those requiring long-term monitoring or involving delicate pathologic animal models.

## Protocol

Necessary experiments to develop the protocol were performed according to national regulations and were approved by the local ethical science committee (Comitato di Bioetica di Ateneo), operating within the institution of University of Turin, Turin, Italy.

# 1. Preparation

1. Anesthesia
    1. Place the animal inside the appropriate isoflurane chamber to anesthetize it.
    2. Fill the chamber with mixed $O_2$ and isoflurane gas for veterinary use at a concentration of 2.5% in a 2 L gas chamber and wait for about 3 min for the rat to fall asleep. Check for the effect of anesthesia by a toe pinch.
    3. Once the anesthesia takes effect, remove the rat and weigh it.
    4. Spread a thin layer of water soluble ophthalmic gel on the animal's eyes to protect them and to maintain the ocular physiological hydration.
    5. Lay the rat down on a ultrasound and photoacoustic imaging station worktop. In order to maintain the anesthesia effect, quickly position the nose inside the appropriate mask providing a constant anesthesia flow (isoflurane 2%-2.5% in oxygen 1 L/min).

2. Shaving the animal
    1. Spread a consistent layer of hair-removing cream on the head surface, with attention to cover areas surrounding ears and neck. Allow the cream to act for several minutes and gently take it out with a spatula. Softly remove all cream remnants with a wet sponge to accurately clean the skin.
    NOTE: The animal fur entraps air that negatively affects ultrasound based imaging acquisition, thus it has to be necessarily removed as much as possible.

3. Positioning the animal
    1. Arrange the animal in a spread-eagle position. Monitor the vital signs, by means of appropriate vital parameter sensors on the worktop (if they are present). Lean the paws on the sensors after applying some drops of electrode cream for professional use.
    NOTE: During anesthesia, ensure that vital parameters have values as follows: rat body temperature ≈ 37.5 °C, cardiac beats per minutes (BPM) varies between 250 and 350 and the respiratory rate is comprised in the range of 40-80 breaths per minute.
    2. Finally fasten the limbs with hypoallergenic artificial silk patch. If necessary, spread again a thin layer of water soluble ophthalmic gel to protect animal's eyes.

# 2. Image Acquisition from Temporal Point of View

1. Positioning the animal
    1. Keeping the animal in a prone position, rotate its body slightly on the side, with a tilt angle of about 45° with respect to the sagittal body axis. Use small cotton gauze rolls as stands to correctly arrange the disposal (**Figure 2a**).
    2. Raise the animal head and rotate it slightly on one side (**Figure 2a**). Use a cotton roll as stand keeping the snout well inserted into the anesthesia mask.
    3. Incline the worktop at an angle of about 30° with respect to the horizontal plane.

4. Turn the imaging transducer at an angle of about 30° with respect to the vertical plane.

2. Ultrasonic and photoacoustic anatomic and vascular image acquisition
    1. Turn the imaging scan on, enter the B Mode image acquisition and properly set all image acquisition parameters to respect possible given requirements of the experiment (**Figure 3a**).
    NOTE: Set the transmit center frequency as low as possible (16 MHz, **Figure 3b**), in order to have the maximum penetration depth possible for the transducer.
    2. Dispose a consistent layer (about 1 cm thick) of hypoallergenic water soluble ultrasound transmission gel on the animal's head (**Figure 2b**). Cover the transducer head with a thin layer of the same gel and put it into contact with the layer on the rat. Use warm gel to minimize localized hypothermia.
    3. Start image acquisition in B Mode and adjust the transducer positioning in real time, by identifying anatomical references and by centering the region of interest to the monitor middle point. Make sure to eliminate air bubbles at any level entrapped into the gel layer, because they negatively affect the acquisition.
    4. Place the transducer to align it to the virtual axis connecting the ear to the eye (**Figure 4a**) to obtain an optimal beam focalization. Acquire different views of the internal brain volume, by clockwise or counterclockwise rotation (**Figure 4b** and **c**).
    5. Eventually fasten the transducer on a mechanical stand to stably secure the position and to tune the orientation in a fine way.
    6. Ensure that the cerebral region of interest localizes at 10 mm of depth with respect to the US-LASER transducer source in order to receive an optimal photoacoustic response signal (**Figure 5**). Then place the indicator of US wave focalization exactly in the center of the analyzed area.
    NOTE: During research of areas of interest, avoid activation of the respiration gate option, in order to accelerate the positioning procedure.
    7. Enter Color Doppler Mode to visualize internal brain blood vessels in a high sensitive way.
    8. Once the positioning has been set in an appropriate way to visualize the wanted regions, activate the respiration gate option to avoid undesired effects related to the movement (**Figure 6a**).
    9. Choose the wanted acquisition parameter set in Color Doppler Mode (**Figure 6b**) and acquire images in this modality to distinguish blood stream velocities and directions, until several millimeters of penetration depth.
    10. Enter Pulsed Wave Doppler Mode and acquire images to detect artery blood pulsation and to differentiate between arteries and veins.
    11. Enter Power Doppler Mode and set acquisition parameters (**Figure 7**) to perform a signal quantification on the basis of the number of scattering events caused by the flux movement, and therefore to evaluated differences in flow rates.
    12. Enter Photoacoustic Mode and properly refine acquisition parameters (**Figure 8a**) to collect data about blood total hemoglobin content or oxygenation degree in a given area. By producing laser excitation on an entire wavelength spectrum (from 680 nm to 970 nm, **Figure 8b**), the absorption of total hemoglobin present in different chemical states inside a tissue can be quantified. By performing signal collection on single specific wavelengths (**Figure 8c**), it is possible to isolate the distinct signal contributions due to the absorption of oxy and de-oxy pure species.

## 3. Imaging from the Occipital Point of View

1. Positioning the animal
    1. Keeping the animal in a prone position, lower the animal head and use small cotton gauze rolls as lateral stands to correctly arrange the disposal.
    2. Turn the imaging transducer parallel to the transverse plane of the animal head (**Figure 9**).
    NOTE: In this way, the acquisition will be centered through the occipital foramen at the basis of the skull. By varying the tilting angle of the probe orientation (**Figure 9**), it will be possible to acquire internal vessel images in different views depending on the setting inclination.

2. Ultrasonic and photoacoustic anatomic and vascular image acquisition
    1. Enter the B Mode image acquisition, set all image acquisition parameters as previously reported (**Figure 3**) and spread the necessary ultrasound gel layers on the probe and on the animal nape.
    2. Arrange the transducer to stay almost horizontal, in order to be directed along the anatomical posterior-to-anterior axis of the body. Point it toward the frontal side of the snout and tilt it slightly forward.
    3. Start image acquisition in B Mode and Color Doppler Mode (**Figures 3** and **6**). Accurately adjust the transducer position and remove air bubbles from the gel coat as previously described. If possible, fasten the transducer on a firm stand to control the orientation in a fine way and choose the best tilting angle to acquire images of the desired anatomical regions.
    4. Visualize internal brain blood vessels in Power Doppler Mode, by properly setting acquisition parameters (**Figure 7**).
    5. Localize intensely pulsated arteries by Pulsed Wave Doppler Mode. Distinguish them from veins, which conversely are characterized by low levels of blood flow pulsation.
    6. Collect blood stream velocities data and directions in Color Doppler Mode, by adequately adapting acquisition parameters (**Figure 6**).
    7. Complete deep brain hemodynamic characterization data set, by adding chemical blood information obtained through the photoacoustic acquisition (**Figure 8**). Perform this by assessing in particular the amount of hematic parameters such as the $O_2$ saturation percentage and the total Hemoglobin content (HbT), that are generally measured by setting the laser excitation wavelength at 750 and 850 nm (**Figure 8c**).

## 4. End of Acquisition and Animal Removal

NOTE: Properly consider the whole time dedicated to the image acquisition process (from step 1 to step 3), which is subjected to main restrictions related to anesthetic dose applied to the animal.

1. Save all acquired data, turn the laser pulsing off by exiting the Photoacoustic acquisition mode and distance the transducer.
2. While maintaining the animal under the anesthesia effect, start to clean it by gently removing the protective gel from the eyes with a wet cotton swab. Use a spatula and several paper towels to completely remove the ultrasound gel from the head and the snout, then clean them with a wet sponge. Be careful not to damage the delicate shaved skin.
3. Take out the adhesive patch used to fasten the limbs and disconnect them from the sensors that monitor the physiologic parameters. Rapidly transfer the animal from the acquisition worktop to a different cage.
4. Host the animal in a small cage for recovery from anesthesia. Ensure that the animals should not share the cage during this phase in order to prevent aggressions
5. Place the recovery cage under an infrared light to keep the animal warm. Wait until it has regained sufficient consciousness to maintain sternal recumbency. Check the animals' general health conditions, before moving it to the animal breeding room.

## Representative Results

This method permits to image both specific anatomic reference structures and blood vessels at relatively high spatial resolution, deeper than the current technique with the animal skin and skull intact. In our experimental conditions the depth of the PA signal is 4.5 mm and the axial resolution is 75 µm with a FOV 23 x 15.5 cm. Experiments with Photoacoustic Tomography modality[19] showed a value of the resolution <1 mm. The range of SNR values is from 21.6 dB to 23.8 dB (obtained by 5 different points randomly selected on the cerebral tissue and background). Juxtaposing the transducer on the skull temporal side, brain images can be acquired as transverse or even coronal sections on the basis of the selected positioning angle of the transducer with a resulting lateral imaging point of view (**Figure 4**). Epidermis, skull bones and parenchymal material are well represented in ultrasonic B-Mode, as they greatly differ in terms of acoustic impendence (**Figure 10**). Even if their configuration depends on the chosen point of view, some anatomical reference sites on parenchyma are recognizable, such as fissures separating brain internal portion from cortex and the characteristic-shaped optic tract (**Figure 10**). Additionally, a large number of vessels are visible both in ultrasonic and photoacoustic imaging modalities. Characteristic intersections of Internal Carotid Artery (ICA) with other main large vessels running along the external lateral surface of the animal's cerebrum can be easily recognized. Large vascular routes, such as the ICA, provide a massive blood supply to satisfy the consistent neuronal need of energy and oxygen. The ICA, originated from Common Carotid Artery (CCA), runs on the lateral side of the head at several millimeters of depth, goes beyond all its bifurcation sites and finally reaches the frontal head portion. This main blood stream spreads among intermediate-sized vessels, before being channeled in always smaller arterioles to finally nourish neurons. From the temporal point of view, it is possible to trace the Internal Cerebral Artery pattern, that bifurcates into vessels directed to front and lateral brain side. Coronal and transverse images can be acquired with different inclination of the transducer with respect to the direction of the virtual axis joining the eye and the auricle of the animal (**Figure 4**). By tilting the transducer according to the projections described in **Figure 4**, it is possible to obtain resolved images of the Middle Cerebral Artery (MCA) that arises from ICA and further divides into two or more branches, that finally surround cortical lobes (**Figures 11** and **12**). The best visualizations were obtained for MCA with the probe tilt as showed in **Figure 4c** and for ICA as showed in **Figure 4b**.

Doppler-based acoustic imaging reveals small branches, while directional information of blood current is available thanks to Color Doppler acquisition (**Figure 13**). MCA artery feature is confirmed by Pulsed Wave ultrasonic technique (**Figures 14** and **15**). Photoacoustic signal of contained hemoglobin into circulating red blood cells can be detected and analyzed to collect data about its molecular oxidative status and to calculate blood oxygen saturation (**Figures 16** and **17**). Hematic oxygen content can be correlated to sonic data in order to confirm the discrimination of arterial blood from venous blood.

By pointing the transducer toward the occipital foramen, the vision is projected on the head axial plane (**Figure 9**) and this imaging plane can be settled on variable inclination angles. In this case, the posterior point of view brain imaging could be connoted by a high penetration depth, because of the larger occipital entry. The Circle of Willis, a characteristic vessel configuration in the deep brain, can be localized and examined by applying all aforementioned techniques. Basilar artery (BA), running on the ventral side of cerebellum, eventually leads to encephalon and symmetrically bifurcates into two branches. These two branches on the ventral brain spread out and then join together again, therefore creating a ring structure (Circle of Willis). This basal deep circle is the vascular basement from which all middle-sized blood vessels arise, such as the Posterior, Middle and Anterior Cerebral Arteries (PCA, MCA and ACA respectively), that are the main effectors of a massive blood supply to the brain. In Color Doppler Mode, the identification of middle sized branches is feasible and enables the clear visualization of curved vascular segments (such as the PCA) entering the Circle of Willis (**Figure 18**).

The cerebral parenchymal tissue was also recorded with PA modality in occipital projection (**Figure 19**) to show vascular characterization in spectral plot (**Figure 20**). With this spectrum is possible distinguish the signal derived from arterial and venous vessels.

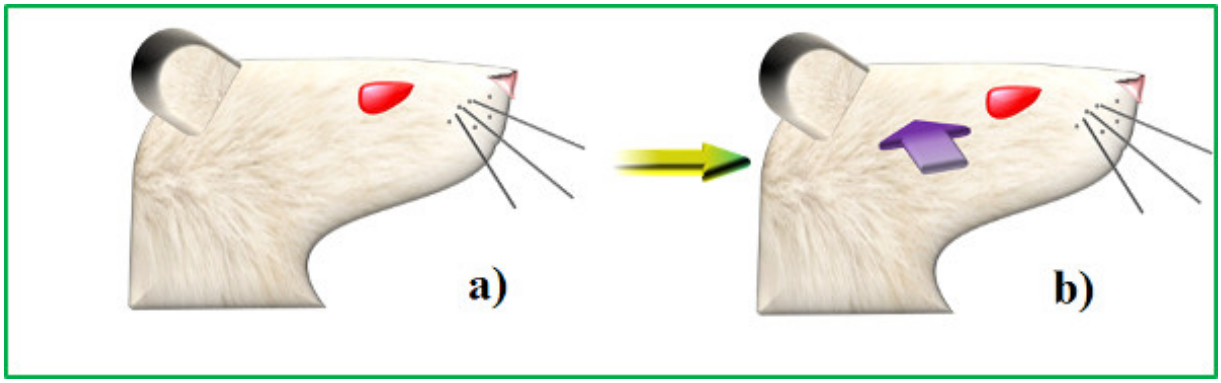


**Figure 1: Location of skull foramina and respective point of view for image acquisition.** The rat head in profile **(a)** and the sites where the imaging transducer device can be placed to be juxtaposed on temporal foramen (purple arrow) and on the occipital foramen (yellow arrow) in profile **(b)**.

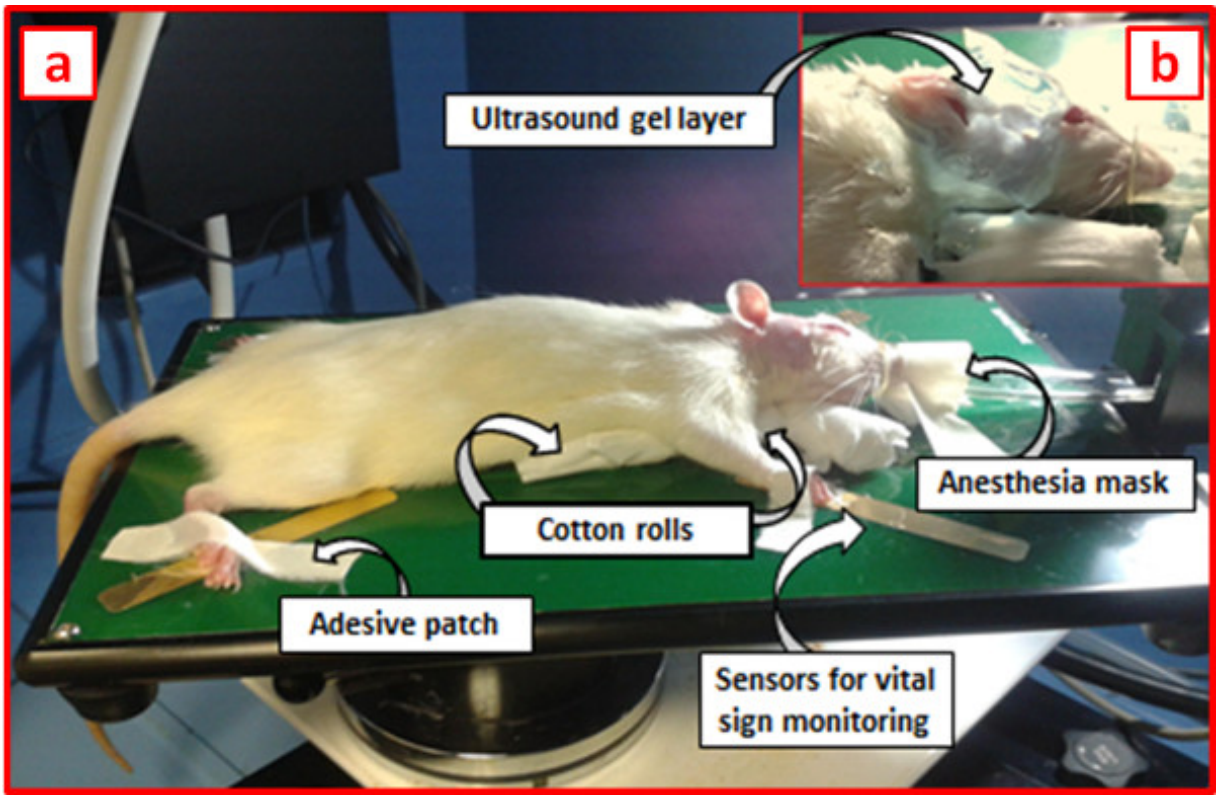


**Figure 2: Animal disposal for temporal image acquisition. (a)** The arrangement of the animal on the worktop for image acquisition: after head shaving, the animal is placed in a prone position with the body slightly tilted on one side in order to expose the temporal side of the head. The worktop may be possibly endowed with a heater device to keep the animal's body warm during acquisition. Some cotton rolls can be used to obtain this position, while adhesive patches fasten the paws on the sensors for vital sign monitoring. **(b)** A consistent layer of ultrasound gel covers the area of the head on which the transducer will be positioned during imaging.

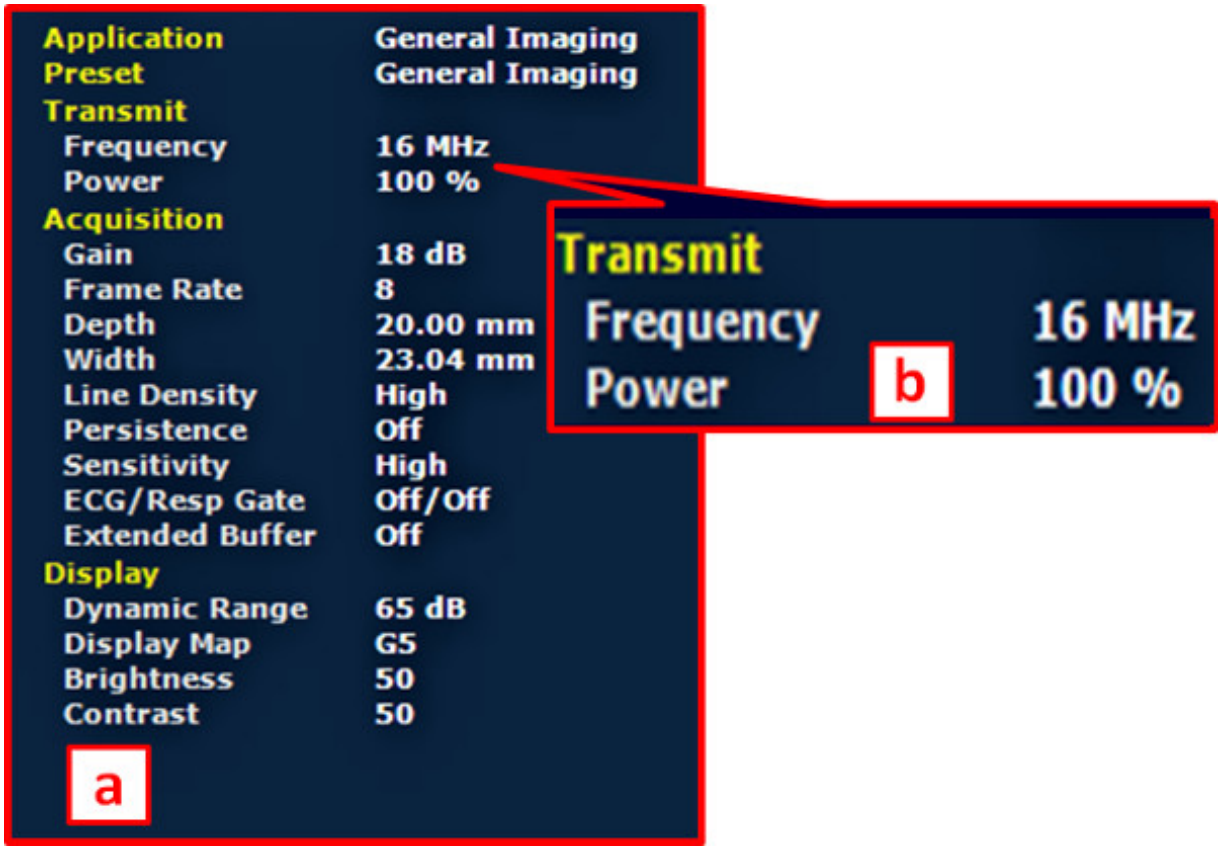


**Figure 3: Acquisition parameters for B-Mode imaging. (a)** An illustrative screenshot showing the panel reporting important acquisition parameters employed for brain imaging in B-Mode. **(b)** Importantly, the transmit frequency was set on low values (16 MHz) to improve US tissue penetration.

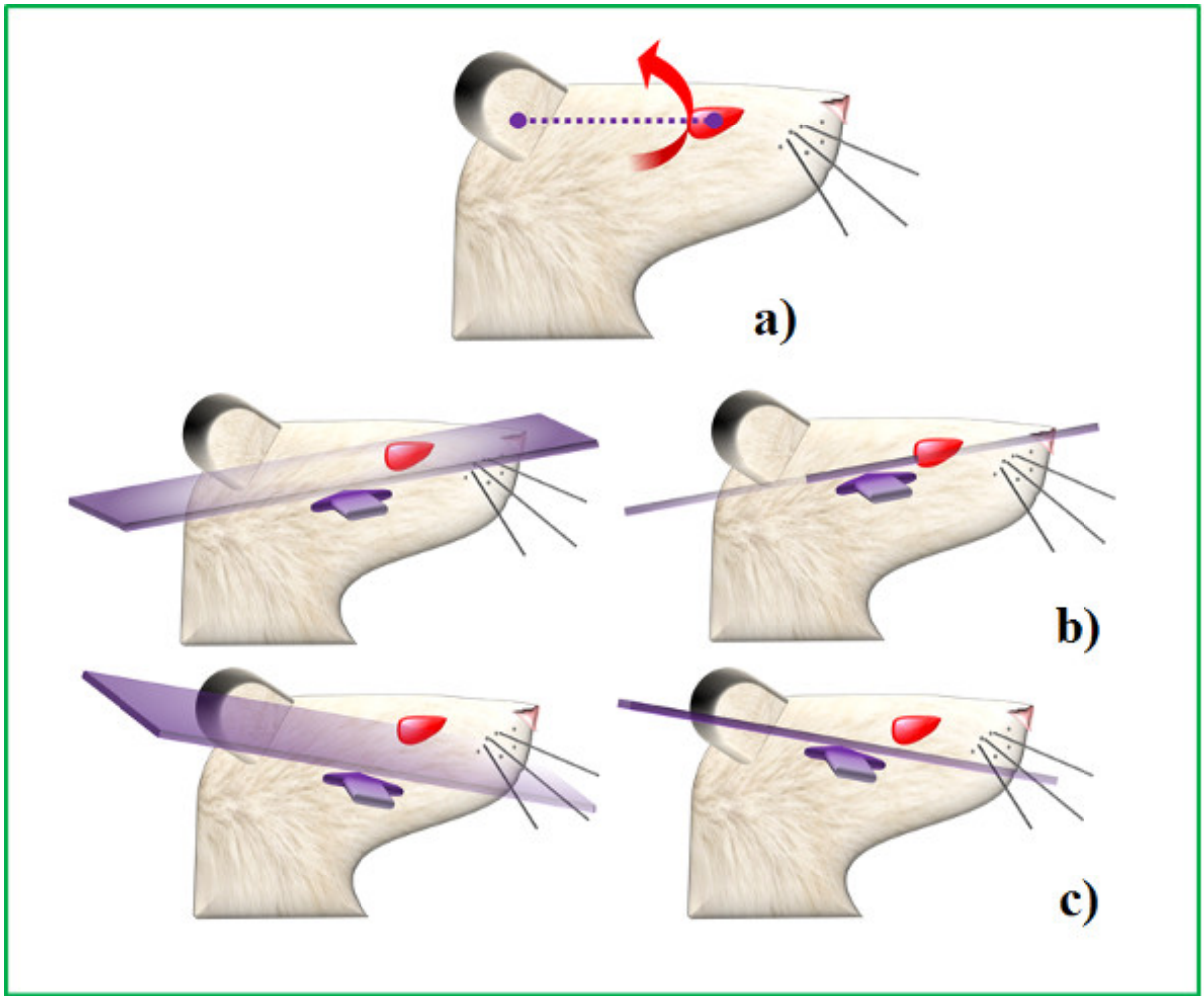


**Figure 4: Transverse image acquisition from temporal foramen. (a)** The virtual reference axis joining the auricle to the eye and the tilt motion (red arrow) to vary the transducer inclination and the image acquisition plane; **(b)** Counterclockwise movement with respect to reference ear-to-eye axis and variable inclination of the transducer position; **c**) Clockwise movement with respect to reference ear-to-eye axis and variable inclination of the transducer position.

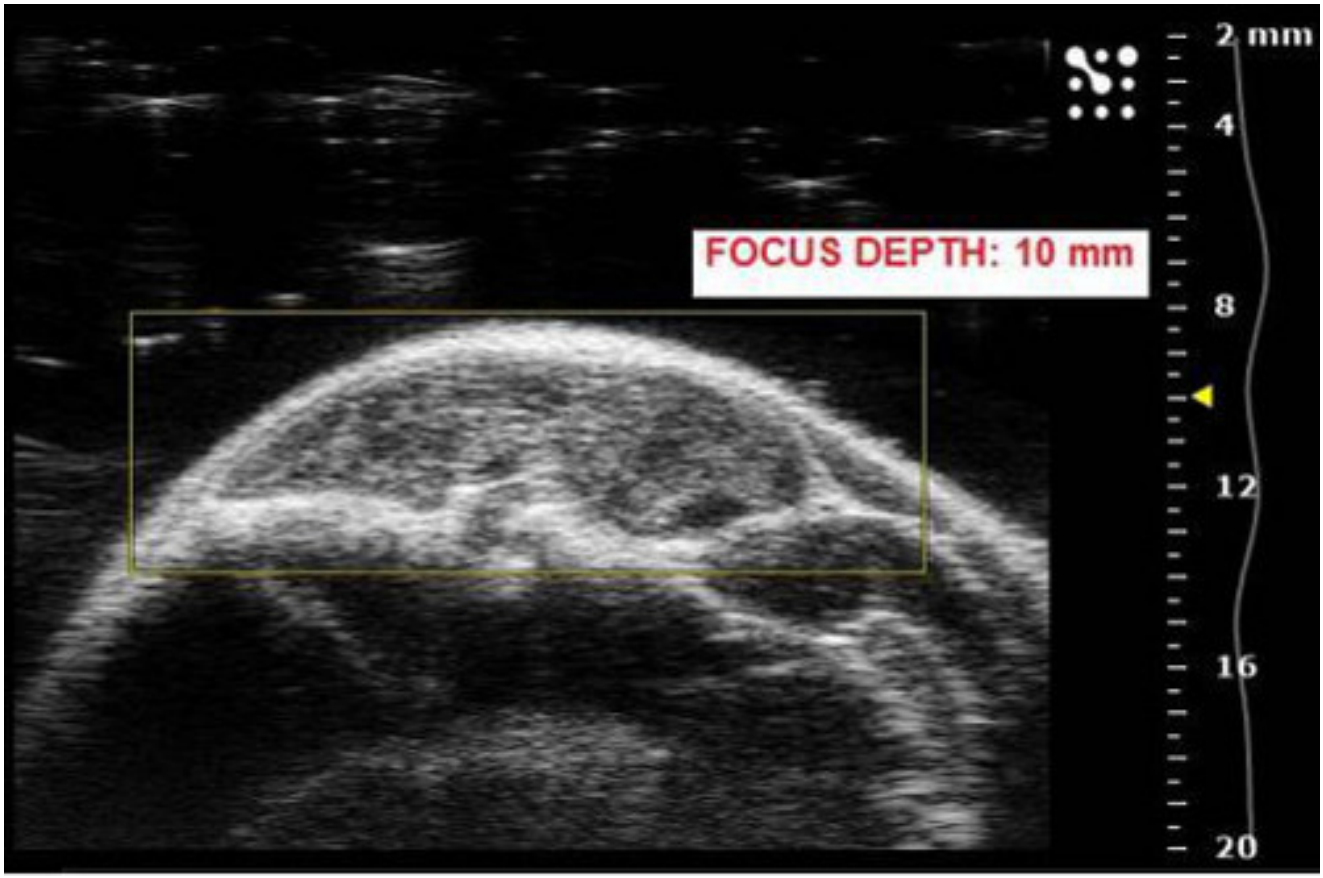


**Figure 5: Optimal focus depth for US and PA image acquisition.** While looking for the area of interest, the imaging focus depth (represented by a yellow triangle) has to be set at around 10 mm of depth from the US/laser source, in order to get an optimal imaging performance.

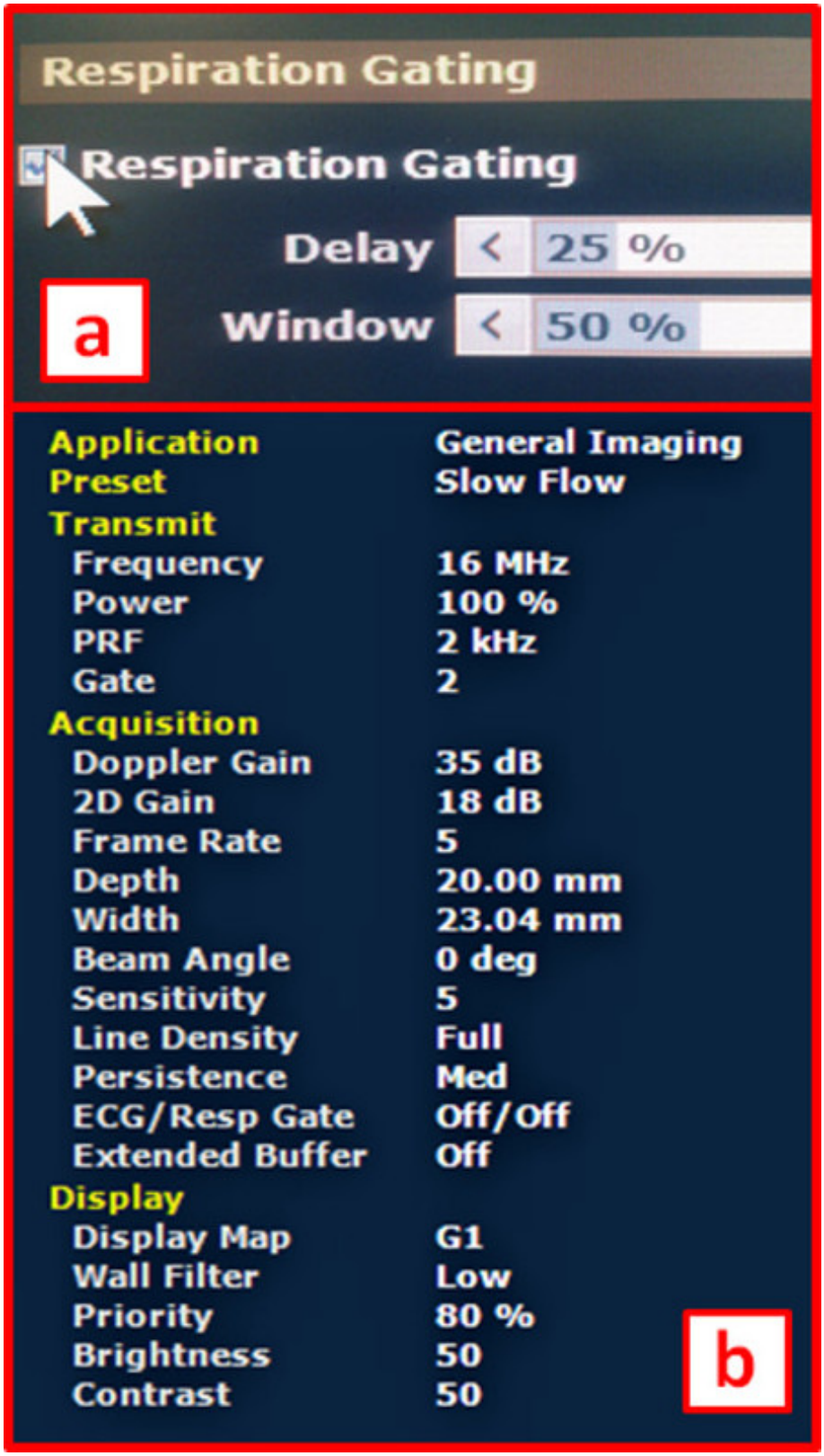


**Figure 6: Acquisition parameters for Color Doppler Mode imaging. (a)** Before starting image acquisition in Color Doppler Mode, the respiration gate option can be turned on, in order to avoid the artifact generated by physiologic respiratory movements. **(b)** An exemplifying screenshot showing important acquisition parameters employed for brain imaging in Color Doppler Mode.

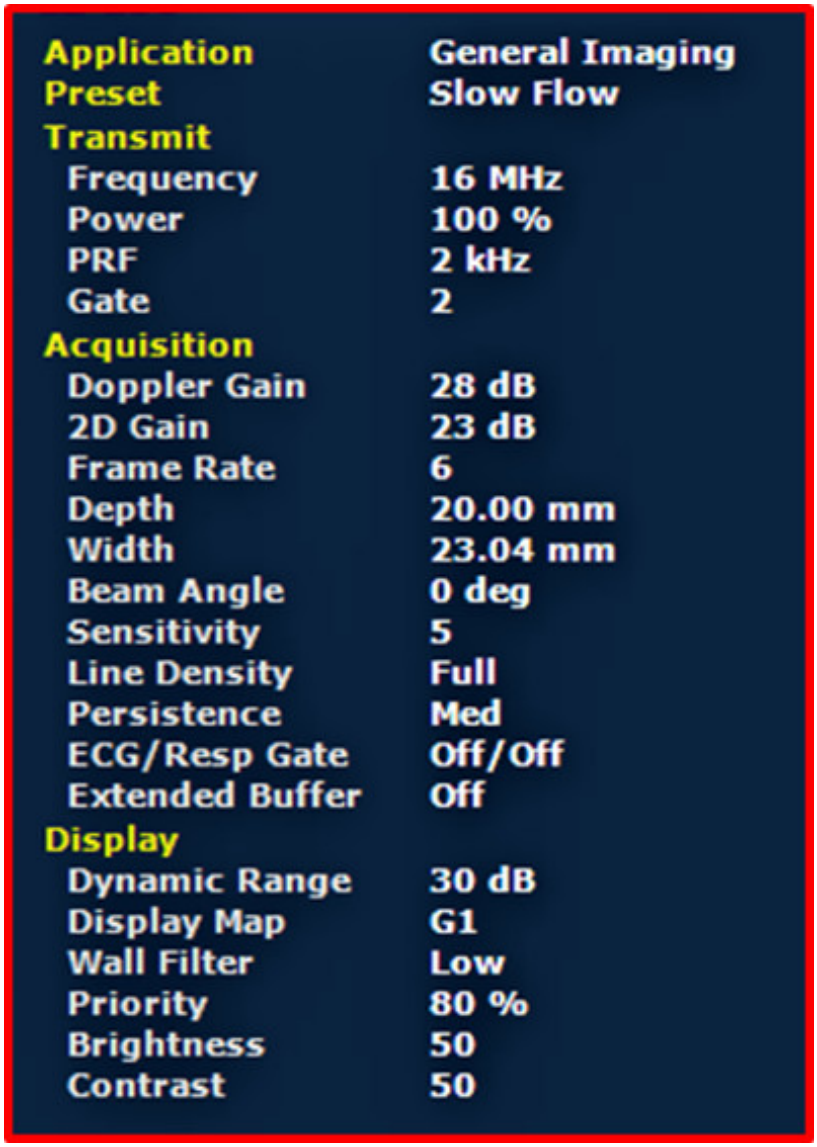


**Figure 7: Acquisition parameters for Power Doppler Mode imaging.** An illustrative screenshot showing important acquisition parameters employed for brain imaging in Power Doppler Mode.

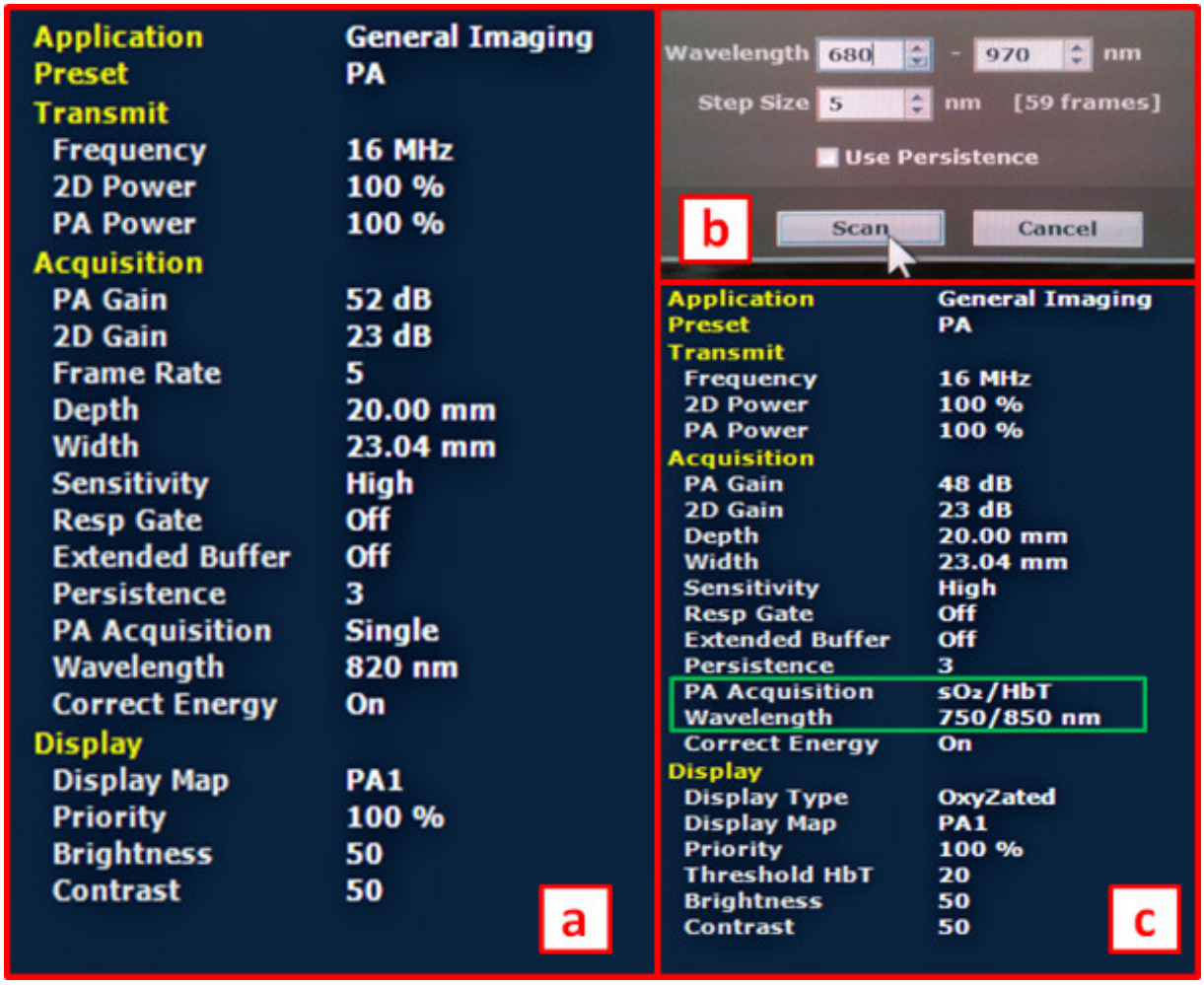


**Figure 8: Acquisition parameters for Photoacoustic Mode imaging. (a)** The panel reporting important acquisition parameters employed for brain imaging in Photoacoustic Mode. **(b)** Acquisition of a Photoacoustic spectrum, based on a laser excitation ranging from 680 nm to 970 nm, with a wavelength interval of 5 nm (referred as step size). **(c)** Acquisition parameters employed for single wave Photoacoustic Mode at 750 nm and 850 nm, for discrimination of de-oxygenated and oxygenated hemoglobin signals respectively.

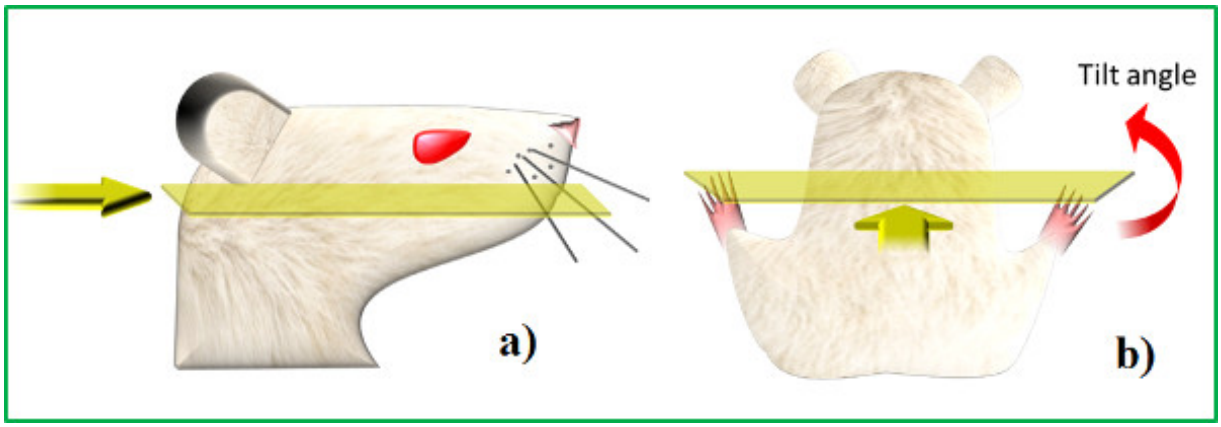


**Figure 9: Transverse image acquisition from occipital foramen. (a)** Transducer positioning on animal's neck (yellow arrow) and the resulting transverse imaging plane that virtually sections the head on the caudo-rostral direction; **(b)** posterior view of the transducer positioning and image acquisition plane.

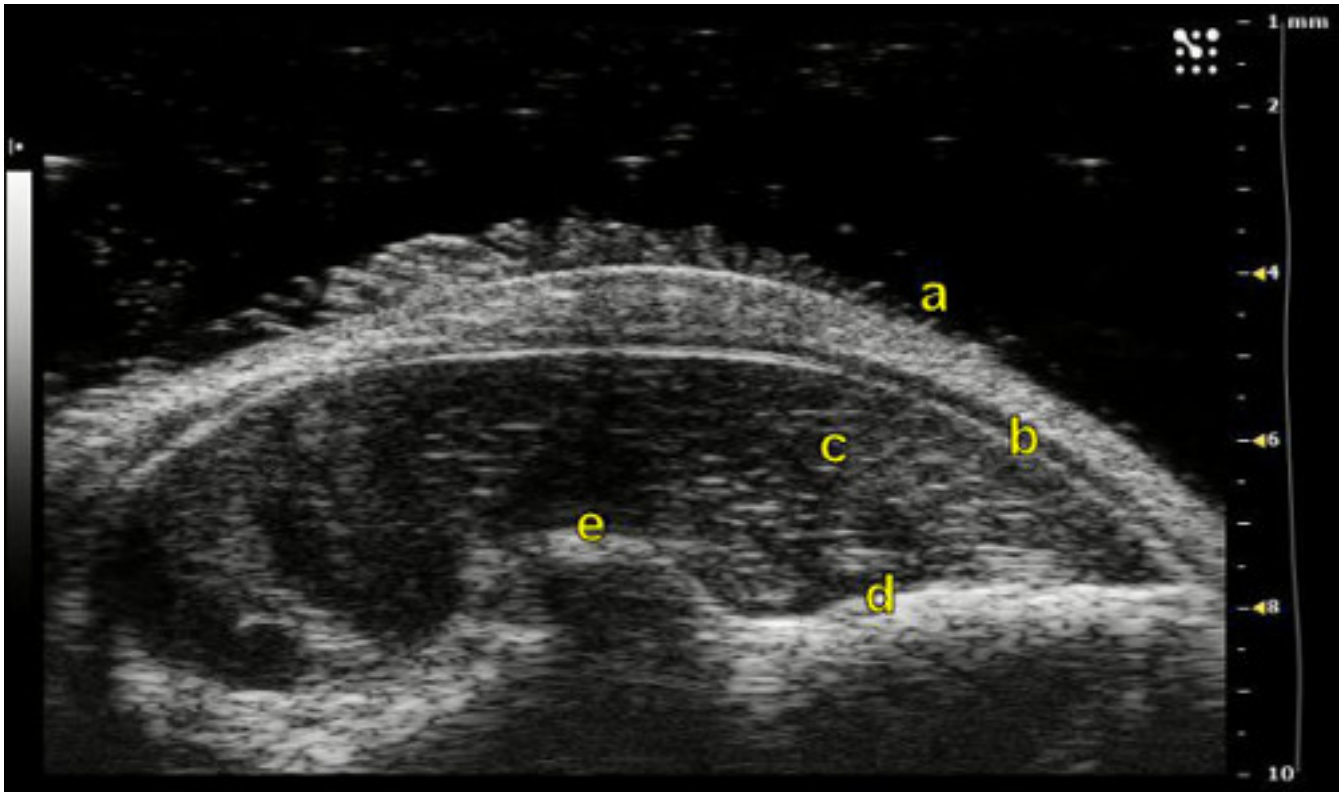


**Figure 10: B-Mode acquisition from temporal foramen for the individuation of anatomic references.** Epidermis **(a)**, skull **(b)** and parenchyma **(c)** can be easily distinguished, but also other anatomic references can be detected, such as the fissure **(d)** surrounding the ventral deep brain portion and the characteristic shape of the optic tract **(e)**.

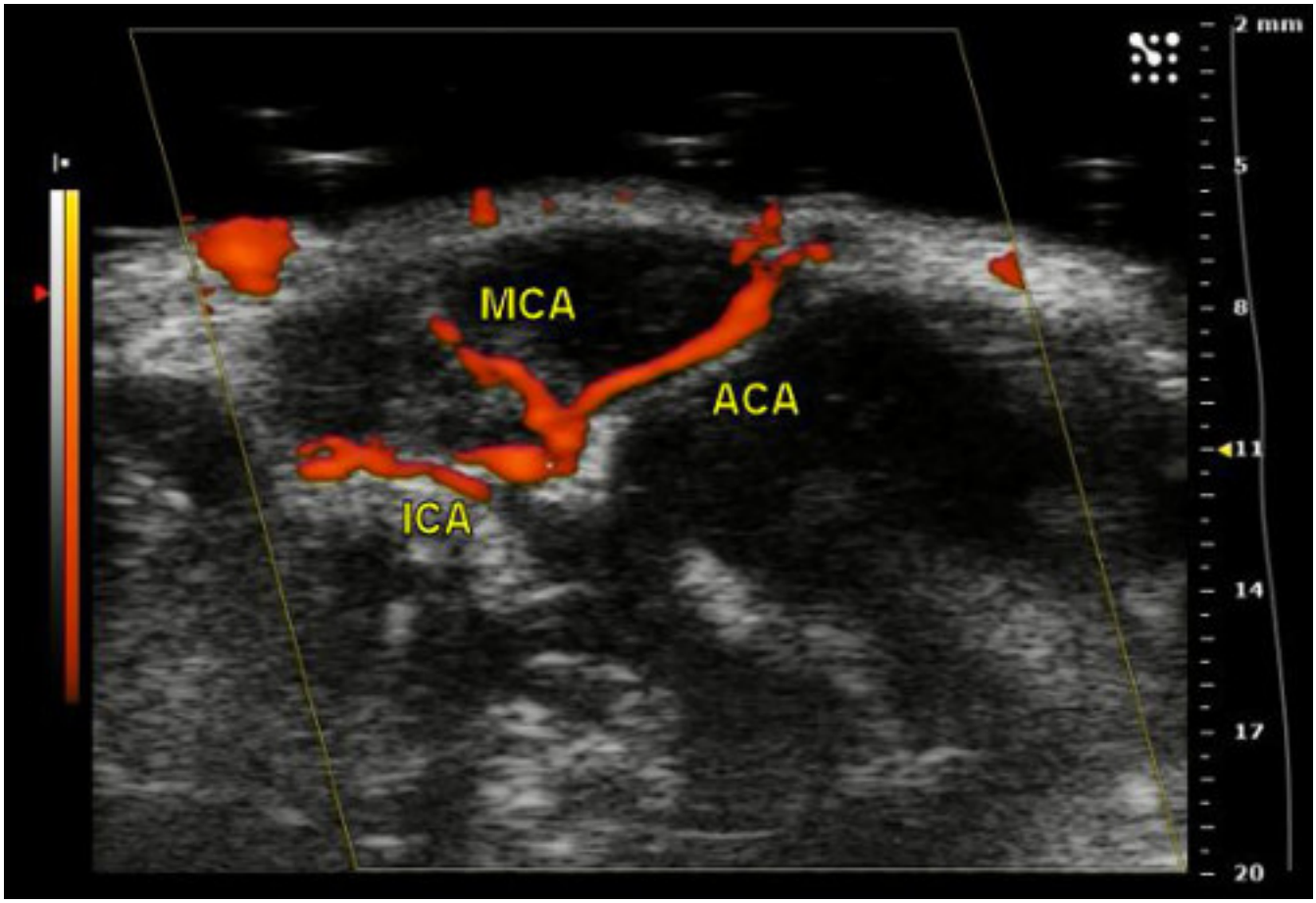


**Figure 11: Power Doppler Mode acquisition through temporal foramen for the individuation of vascular references.** MCA raising from the ICA on the temporal brain side. To obtain this view, transverse image was acquired by pointing the transducer onto the temporal foramen and by rotating it in counterclockwise direction.

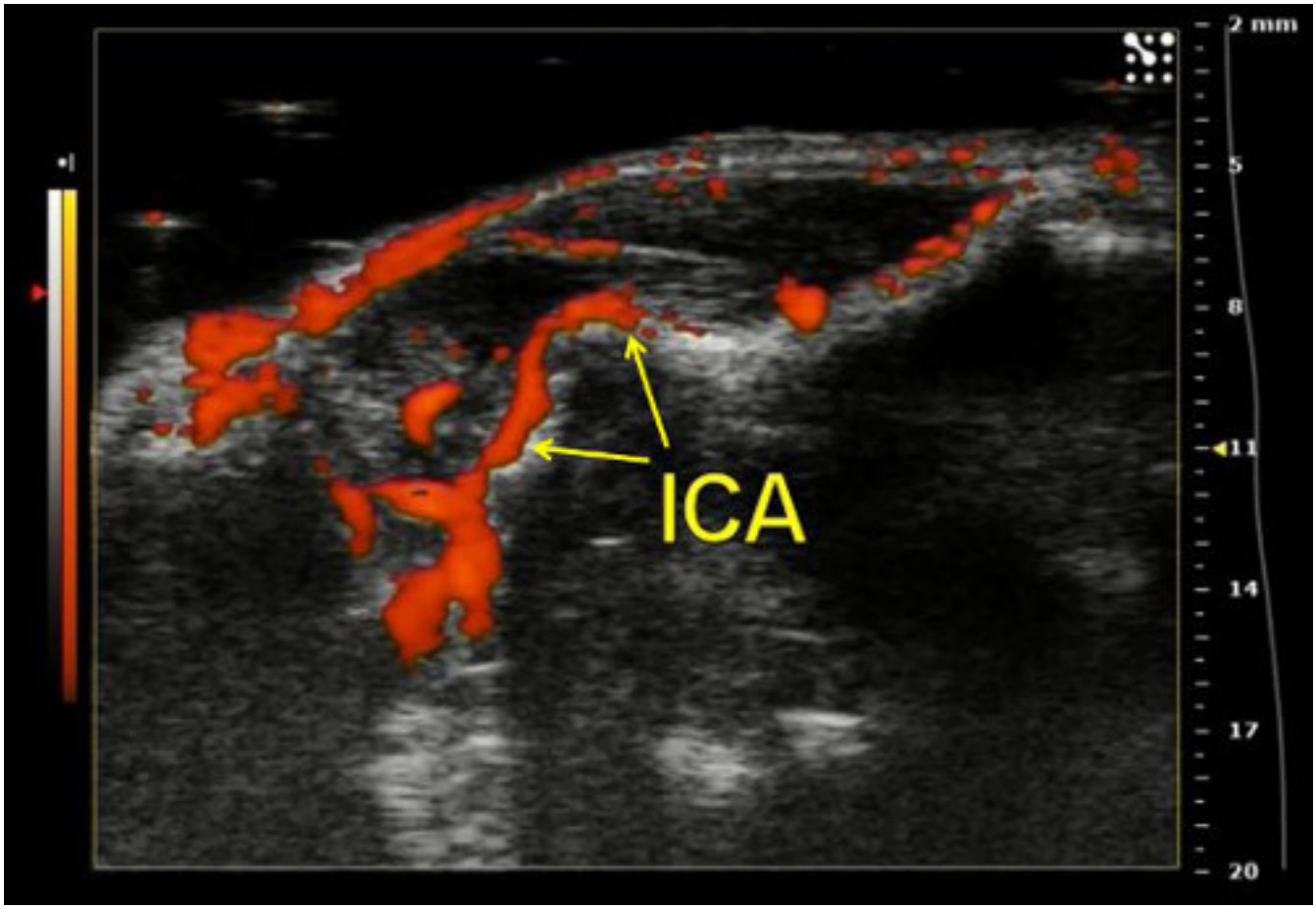


**Figure 12: Power Doppler Mode acquisition through temporal foramen for the individuation of vascular references.** MCA raising from the ICA on the temporal brain side. To obtain this view, transverse image was acquired by pointing the transducer onto the temporal foramen and by rotating it in clockwise direction.

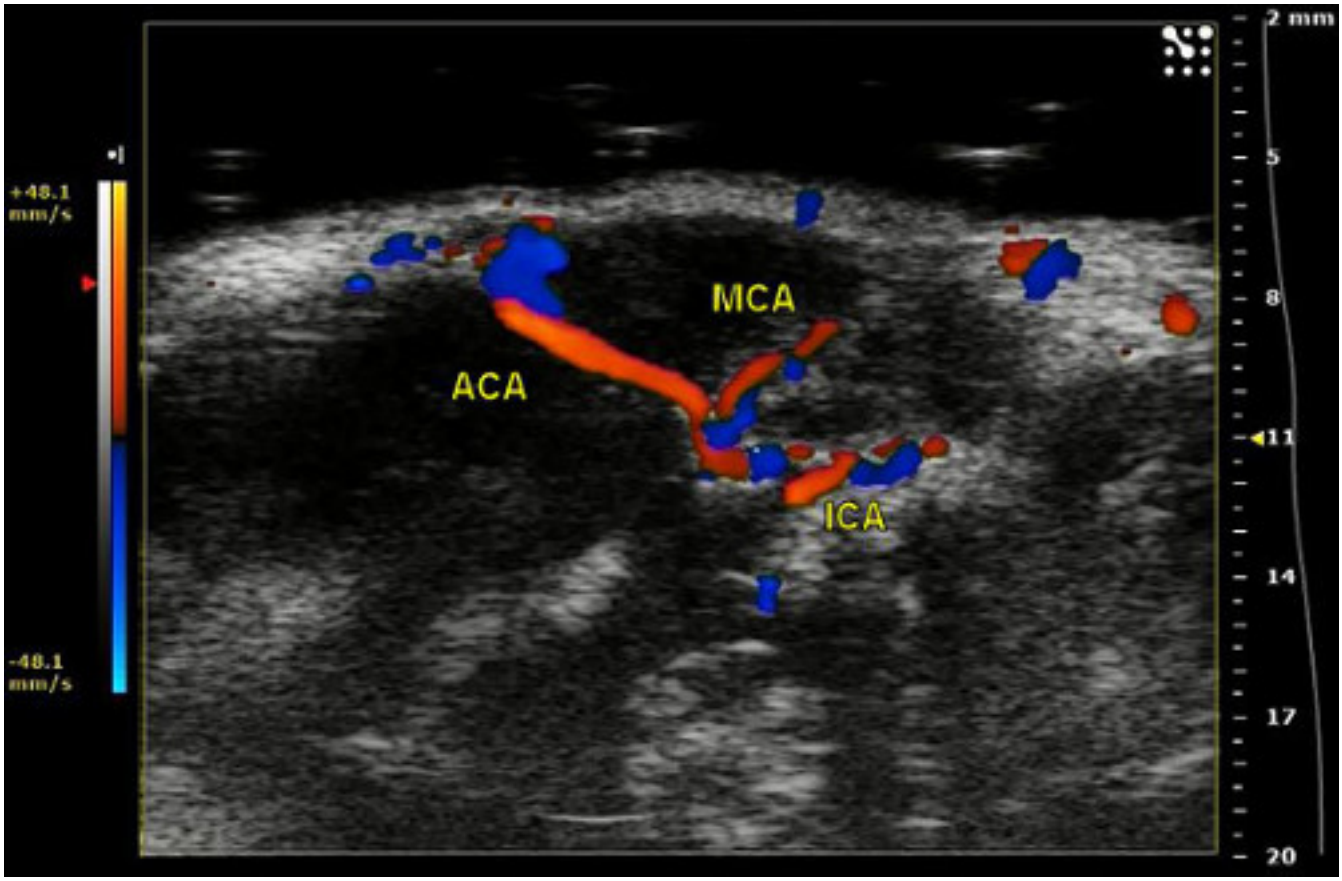


**Figure 13: Color Doppler Mode acquisition through temporal foramen for the individuation of vascular references.** MCA raising from the ICA on the temporal brain side. Directional information of blood stream is expressed by means of a color scale bar, distinguishing between flux movements directed towards the transducer device and away from it.

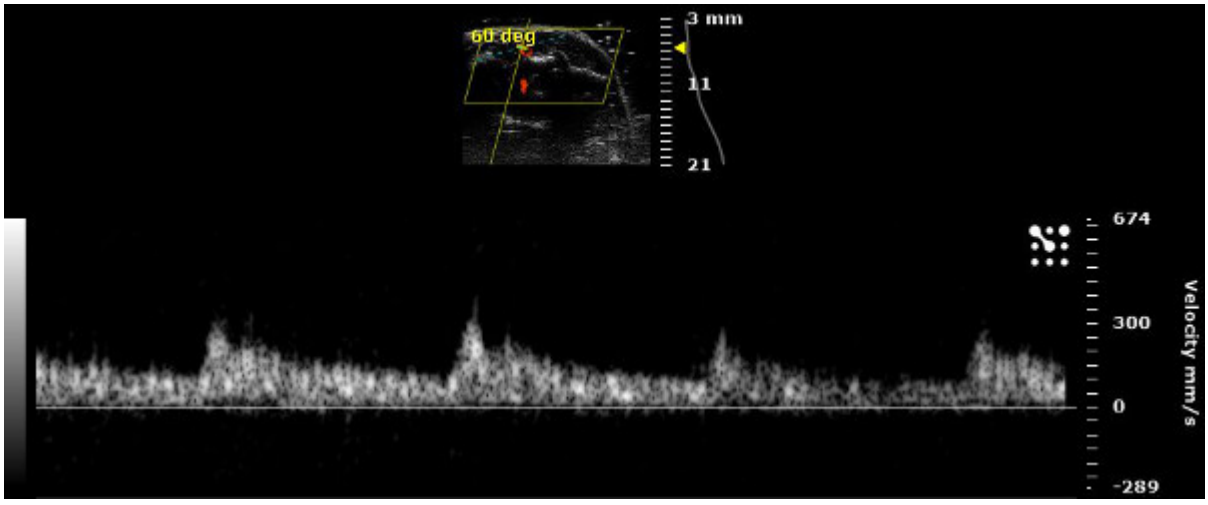


**Figure 14: Pulsed Wave Mode acquisition through temporal foramen for the individuation of vascular references.** Confirmation of the arterial properties of blood circulating inside vessels that were hypothetically identified as arteries: Pulsed Wave Mode provides information about the variation of stream velocities, which can be correlated to cardiac pulsation effect (more intense in arteries than in veins).

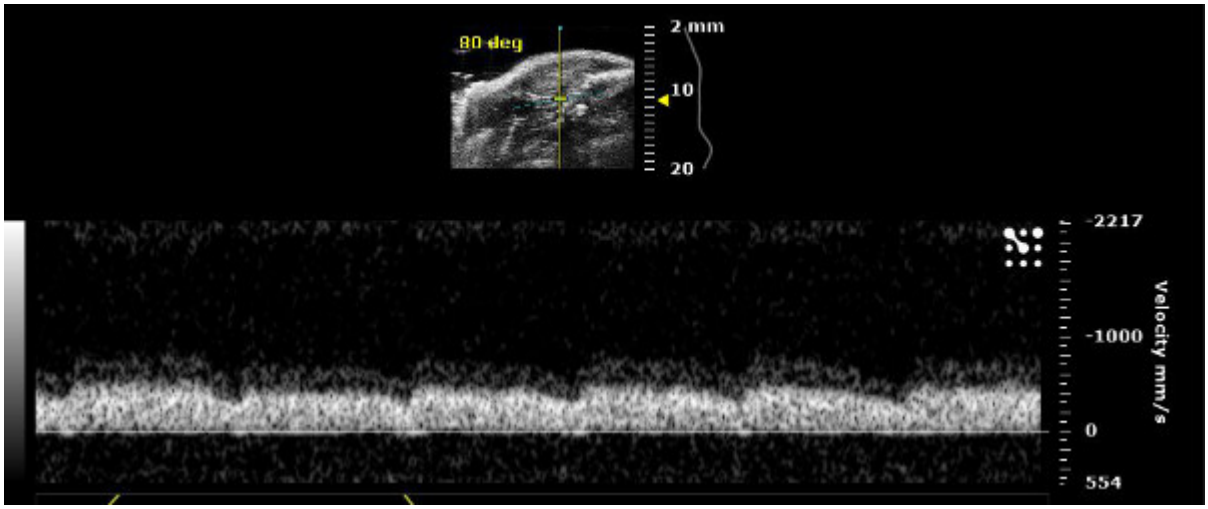


**Figure 15: Pulsed Wave Mode acquisition through temporal foramen for the individuation of vascular references.** Identification by Pulsed Wave Mode of blood vessels as veins, where the cardiac pulsation effect on stream velocities is negligible.

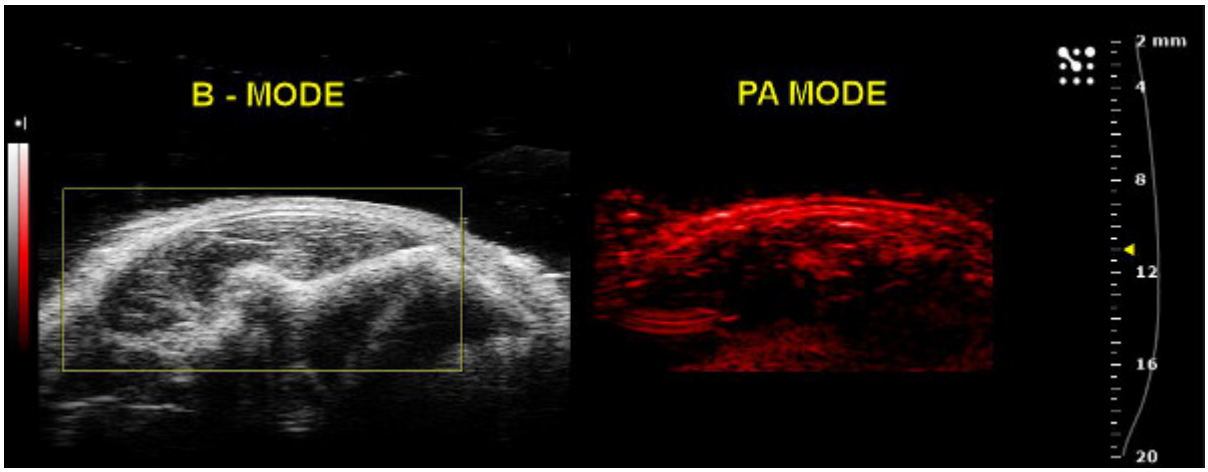


**Figure 16: Photoacoustic Mode acquisition through temporal foramen for the individuation of vascular references**. Parenchymal internal vessels in the temporal brain side visualized by B-Mode (left) and Single-wave Photoacoustic Mode (right). The scale bar colors reflect different intensity values of photoacoustic signal, induced by a laser excitation performed at one selected wavelength. In order to individuate veins and arteries, excitation wavelengths can be set at 750 and 850 nm, representing the values to obtain the photoacoustic emission peaks for deoxygenated and oxygenated hemoglobin respectively.

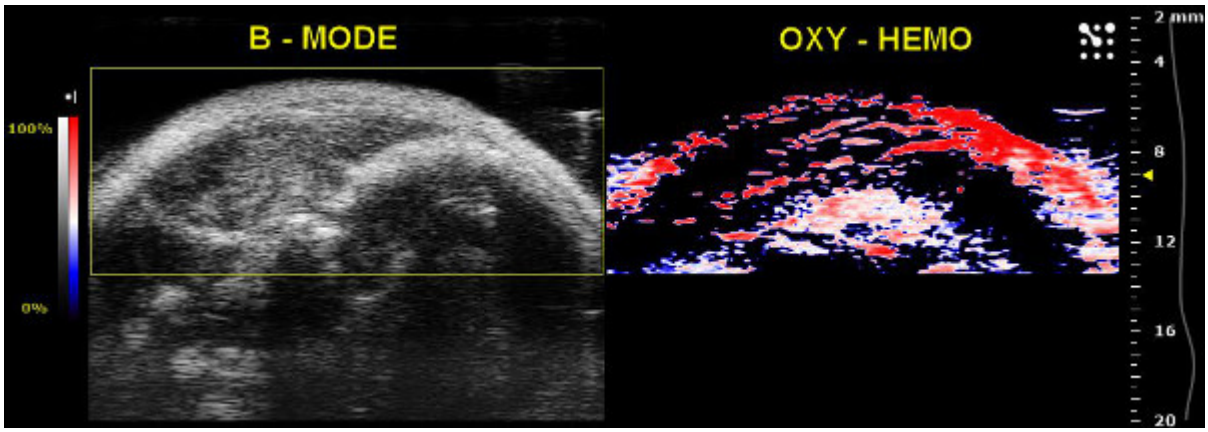


**Figure 17: Photoacoustic Mode acquisition through temporal foramen for oxygenated and de-oxygenated hemoglobin discrimination**. Internal vessels in the temporal brain side visualized by B-Mode (left) and Oxy-Hemo Photoacoustic Mode (right). The scale bar colors reflect different percentage values of oxygen saturation of blood hemoglobin.

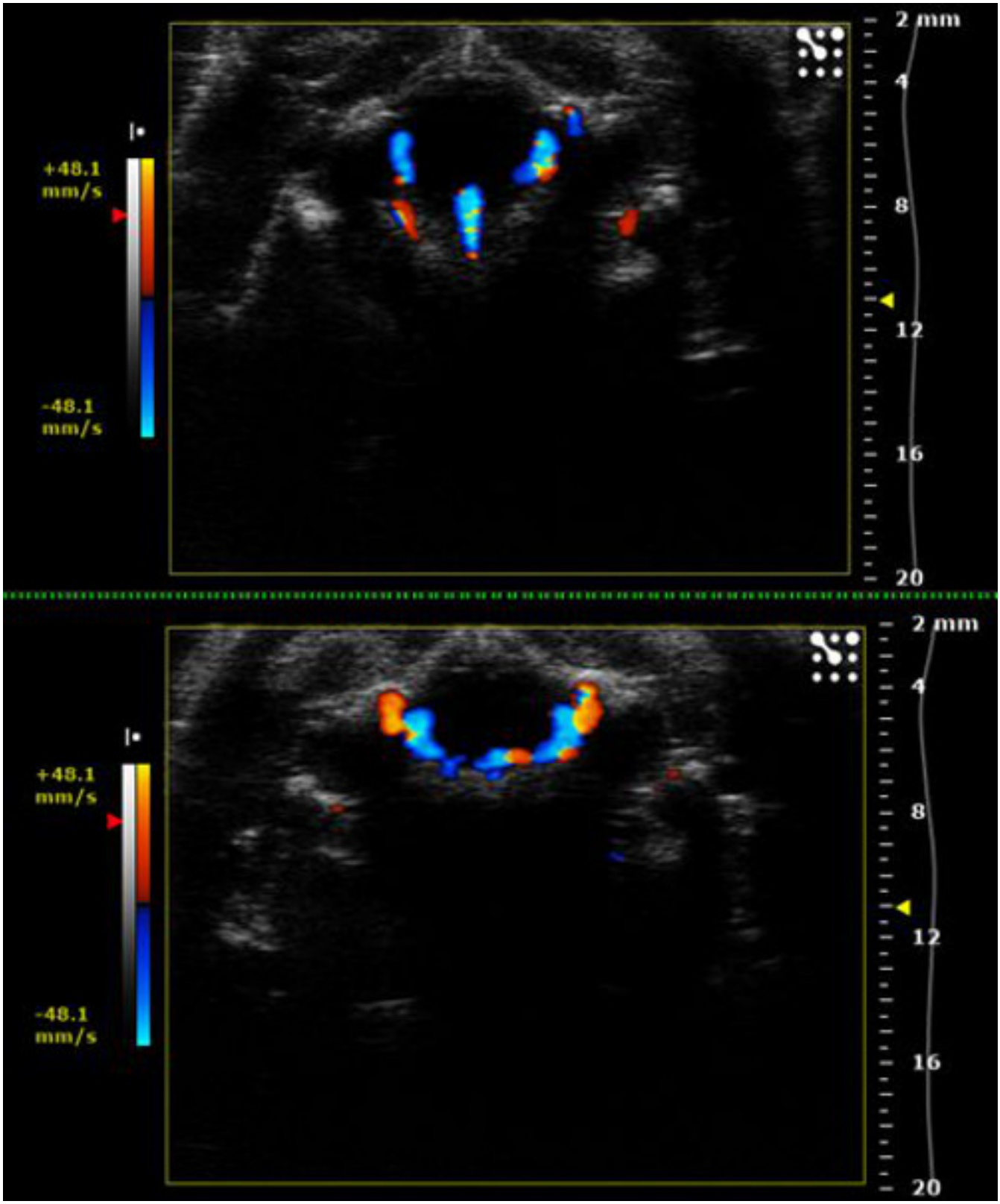


**Figure 18: Color Doppler Mode acquisition through occipital foramen for the individuation of vascular references**. Curved vascular segments creating the basement structure of the Circle of Willis, located in the ventral brain side.

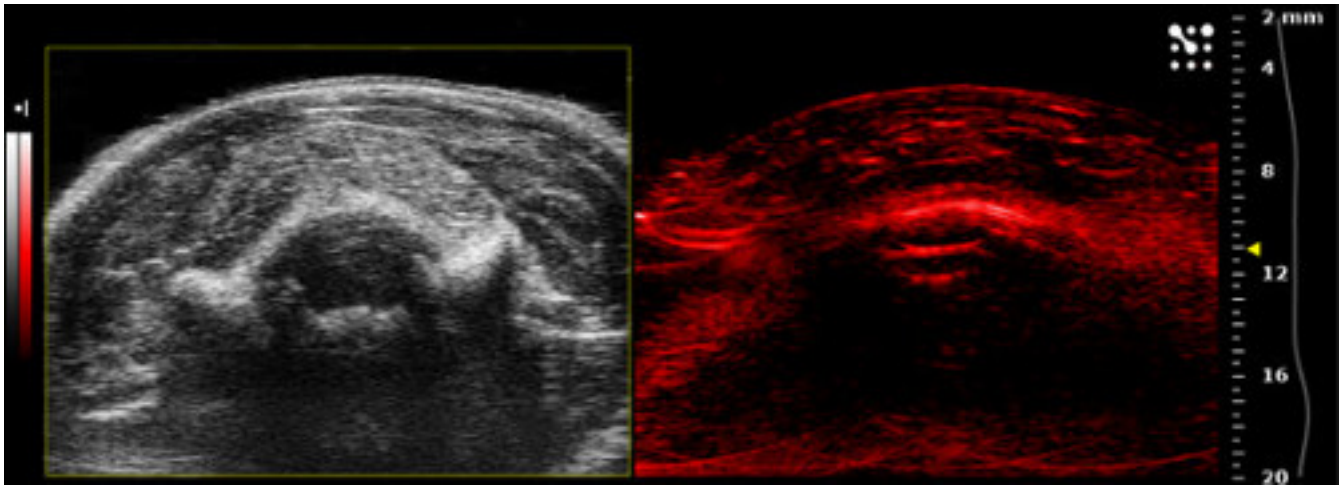


**Figure 19: Photoacoustic and B-Mode acquisition through occipital foramen for the individuation of vascular references**. Nell'immagine in B-mode si possono evidenziare le strutture anatomiche individuabili con la proiezione occipitale e nella corrispondente acquisizione con modalità fotoacustica con rilevamento spettrale tra 670 nm a 980 nm (con step di 5 nm).

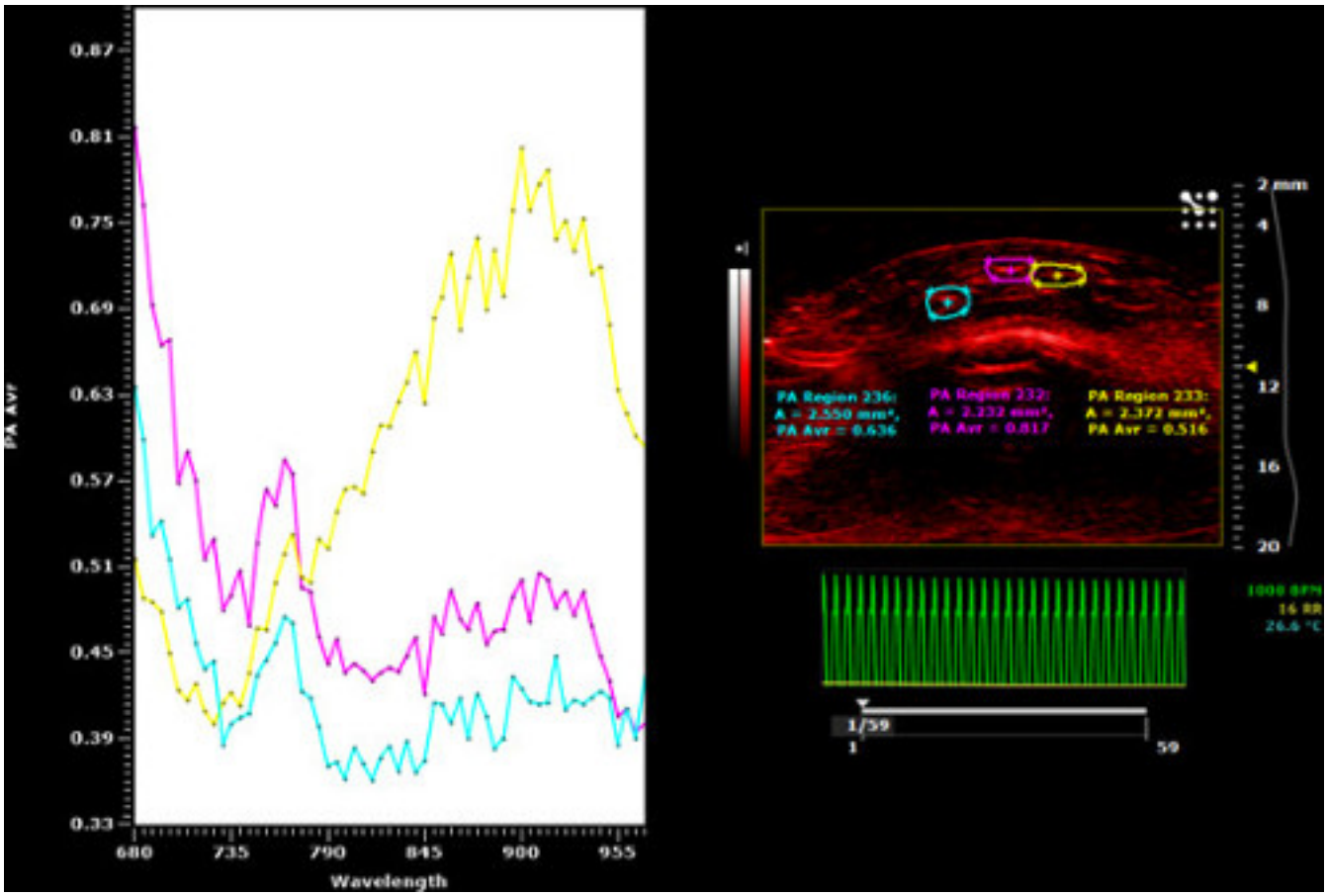


**Figure 20: Photoacoustic and B-Mode acquisition through occipital foramen for the individuation of vascular references**. In questa imagine viene rappresentato lo spettro corrispondente alle tre ROIs tracciate a livello del parenchima cerebellare; in particolare sono tracciate a livello di tre strutture vascolari, la cui tipologia si differenzia a livello dell'andamento spettrale (ROIs fuxia e celeste corrispondono a strutture vascolari venose; ROI gialla corrisponde ad una struttura vascolare arteriosa).

## Discussion

The presented protocol was optimized in order to provide highly effective brain imaging performance in small animals. Images can be acquired in different modalities by precisely following the indications about the acquisition parameters and the transducer positioning on skull foramina. In particular, the positioning on the temporal side is the most critical, since the US and the laser have to be centered as precisely as possible to

correctly penetrate the foramen, which is smaller than the occipital one. Nevertheless, thanks to this experimental setting, hemodynamic features related to physiologic or even pathologic contests are accessible and can be evaluated even in deep brain regions, which are usually difficult to characterize.

Since successful image acquisition depends on the accuracy of the transducer positioning, this dependence has to be carefully taken into account because it may affect the imaging performance. For instance, some anatomical structures of interest could be not completely included in the acquisition imaging plane and their identification from images that offer just a partial vision could result suboptimal. Moreover, an US and PA imaging acquisition performed in a three-dimensional modality (3D Mode) would be not compatible with the previously described experimental setting, since it requires the transducer to move along a pre-defined automatized path. Finally, due to the natural anatomic variability, the dimension of skull openings may significantly vary among animals, thus having unpredictable repercussions on the acquisition process. This fact makes the image quality dependent on the characteristics of each individual. Consequently, the impossibility to apply this strategy to some animals has to be considered when designing the experimental protocol.

Specifically, a remarkable interest is addressed to hemodynamics, due to its fundamental role in determining the biodistribution of drugs or other exogenous molecules after systemic administration[28-29]. The applicative implications in the field of Molecular Imaging are many, ranging from the validation of blood pool imaging contrast agents to image-monitored drug delivery studies requiring ultrasound-induced BBB opening[30]. All of these research purposes will certainly benefit from the minimal invasiveness of the protocol, considering that, without any additional surgery, the risk of death or unwanted side effects is substantially reduced and long-term monitoring on the same animal models is feasible.

In summary, the presented protocol will enable the practitioner to efficiently image and correctly interpret the anatomic topography and the vascular pattern of normal or pathologic brain tissues in research-use animal models. While current methods are mainly limited to tomographic cortical imaging[25-27], this setting gives the opportunity to illustrate several processes that influence deep brain physiology, by merging advantages provided by both US and PA imaging.

## Disclosures

Publication fees for this article were sponsored by Visual Sonics.

## Acknowledgements

The authors have no acknowledgements.

## References

1. Bestmann, S., Feredoes, E. Combined neurostimulation and neuroimaging in cognitive neuroscience: past, present, and future. *Ann N Y Acad Sci.* **1296**, 11-30 (1111).
2. Kim, S. A., Jun, S. B. In-vivo Optical Measurement of Neural Activity in the Brain. *Exp Neurobio.* **22**, (3), 158-166 (2013).
3. Silva, G. A. Nanotechnology approaches to crossing the blood-brain barrier and drug delivery to. *the CNS.BMC Neurosci.* **9**, Suppl 3. S4 (2008).
4. Stemmer, N., Mehnert, J., Steinbrink, J., Wunder, A. Noninvasive fluorescence imaging in animal models of stroke. *Curr Med Chem.* **19**, (28), 4786-4793 (2012).
5. Frohman, E. M., Fujimoto, J. G., Frohman, T. C., Calabresi, P. A., Cutter, G., Balcer, L. J. Optical coherence tomography: a window into the mechanisms of multiple sclerosis. *Nat Clin Pract Neurol.* **4**, (12), 664-675 (2008).
6. Liao, L. D., *et al.* Neurovascular coupling: in vivo optical techniques for functional brain imaging. *Biomed Eng Online.* 12-38 (2013).
7. Youn, H., Hong, K. J. In vivo Noninvasive Small Animal Molecular Imaging. *Osong Public Health Res Perspect.* **3**, (1), 48-59 (2012).
8. Miyawaki, A.Fluorescence imaging in the last two decades. *Microscopy (Oxf).* **62**, (1), 63-68 (1093).
9. Feldman, M. K., Katyal, S., Radiographics Blackwood, M. S. U. S. artifacts **29**, (4), 1179-1189 (1148).
10. Postema, M., Gilja, O. H. Contrast-enhanced and targeted ultrasound. *World J Gastroenterol.* **17**, (1), 28-41 (2011).
11. Zacharatos, H., Hassan, A. E., Qureshi, A. I. Intravascular ultrasound: principles and cerebrovascular applications. *AJNR Am J Neuroradiol.* **31**, (4), 586-597 (2010).
12. Li, C., Wang, L. V. Photoacoustic tomography and sensing in biomedicine. *Phys Med Biol.* **54**, (19), R59-R97 (2009).
13. Kim, C., Favazza, C., Wang, L. V. In vivo photoacoustic tomography of chemicals: high-resolution functional and molecular optical imaging at new depths. *Chem Rev.* **110**, (5), 2756-2782 (2010).
14. Hu, S., Wang, L. V. Photoacoustic imaging and characterization of the microvasculature. *J Biomed Opt.* **15**, (1), (2010).
15. Mallidi, S., Luke, G. P., Emelianov, S. Photoacoustic imaging in cancer detection, diagnosis, and treatment guidance. *Trends Biotechnol.* **29**, (5), 213-221 (2011).
16. Pysz, M. A., Gambhir, S. S., Willmann, J. K. Molecular imaging: current status and emerging strategies. *Clin Radiol.* **65**, (7), 500-517 (2010).
17. Nie, L., Cai, X., Maslov, K., Garcia-Uribe, A., Anastasio, M. A., Wang, L. V. Photoacoustic tomography through a whole adult human skull with a photon recycler. *J Biomed Opt.* **17**, (11), (2012).
18. Huang, C., *et al.* Aberration correction for transcranial photoacoustic tomography of primates employing adjunct image data. *J Biomed Opt.* **17**, (6), (2012).
19. Nie, L., Guo, Z., Wang, L. V. Photoacoustic tomography of monkey brain using virtual point ultrasonic transducers. *J Biomed Opt.* **16**, (7), (2011).
20. Guevara, E., *et al.* Imaging of an inflammatory injury in the newborn rat brain with photoacoustic tomography. *PLoS On.* **8**, (12), (2013).
21. Yao, J., Wang, L. V. Photoacoustic Microscopy. *Laser Photon Rev.* **7**, (5), (2013).
22. Liu, Y., *et al.* Assessing the effects of norepinephrine on single cerebral microvessels using optical-resolution photoacoustic microscope. *J Biomed Opt.* **18**, (7), (2013).

23. Xia, J., *et al.* Whole-body ring-shaped confocal photoacoustic computed tomography of small animals in vivo. *J Biomed Opt.* **17**, (5), 050506 (2012).
24. Sun, J., Lindvere, L., Van Raaij, M. E., Dorr, A., Stefanovic, B., Foster, F. S. In vivo imaging of cerebral hemodynamics using high-frequency micro-ultrasound. *Cold Spring Harb Protoc.* (9), (2010).
25. Nasiriavanaki, M., Xia, J., Wan, H., Bauer, A. Q., Culver, J. P., Wang, L. V. High-resolution photoacoustic tomography of resting-state functional connectivity in the mouse brain. *Proc Natl Acad Sci U S A.* **111**, (1), 21-26 (2014).
26. Jao, J., *et al.* Noninvasive photoacoustic computed tomography of mouse brain metabolism in vivo. *Neuroimage.* **64**, 257-266 (2013).
27. Deng, Z., Wang, Z., Yang, X., Luo, Q., Gong, H. In vivo imaging of hemodynamics and oxygen metabolism in acute focal cerebral ischemic rats with laser speckle imaging and functional photoacoustic microscopy. *J Biomed Op.* **17**, (8), 081415-081414 (2012).
28. Huang, R. B., Mocherla, S., Heslinga, M. J., Charoenphol, P., Eniola-Adefeso, O. Dynamic and cellular interactions of nanoparticles in vascular-targeted drug delivery. *Mol Membr Biol.* **27**, (7), 312-327 (2010).
29. Saxer, T., Zumbuehl, A., Müller, B. The use of shear stress for targeted drug delivery. *Cardiovasc Res.* **99**, 328-3233 (2013).
30. Zhao, Y. Z., Lu, C. T., Li, X. K., Cai, J. Ultrasound-mediated strategies in opening brain barriers for drug brain delivery. *Expert Opin Drug Deliv.* **10**, 987-1001 (2013).